Measurements of a Planar Nine-Way Metamaterial Power-Combined Amplifier

Wei-Chiang Lee* and Tah-Hsiung Chu
Department of Electrical Engineering, National Taiwan University, Taipei, Taiwan

***Abstract* —In this paper, measurement results of a planar nine-way metamaterial power-combined amplifier are presented. The power-divider/combiner structure is a metamaterial lens composed of positive refractive index (PRI) material with right-handed unit cells and zero refractive index (ZRI) material with left-handed unit cells. Due to its uniform isolation characteristics, the graceful degradation performance of this power-combined amplifier is shown to be independent of the amplifier failure sequence. The power combining of nine 1-W amplifiers gives an output power of 7.64 W with a combining efficiency of 85% at 1.008 GHz, and the graceful degradation characteristic of this power-combined amplifier is experimentally demonstrated.[1]**

I. INTRODUCTION

Due to the power capacity of solid-state devices, power combining of multiple devices becomes necessary as a higher output power level is required. Therefore, development of microwave power-dividing/combining techniques [1] of solid-state devices to achieve low loss and high combining efficiency is desirable. As the number of active devices increases, *N*-way power-dividing/combining structures, such as Wilkinson [2] and radial [3], [4] structures in a parallel configuration, are usually used due to compactness. These structures do not have the disadvantage of increasing loss with the number of active devices existed in chain [5] and tree [6] configurations. However, their main problem is having non-collinearly aligned multiple ports to make their integration with active devices in a planar structure difficult.

Recently, metamaterials with negative refractive index having left-handed (LH) propagation behavior are extensively applied to microwave devices [7]. Specifically, they are mainly composed of one-dimensional right-handed (RH) and LH transmission lines called composite right/left-handed (CRLH) transmission lines [8]. By properly operating CRLH transmission lines at the infinite wavelength frequency, metamaterials can have a zero-phase shift characteristic along the structure to give an equal magnitude and phase distribution [9]. Based on this characteristic, planar [10], [11] metamaterial power dividers using positive refractive index (PRI) material and zero refractive index (ZRI) material are presented. Specifically, the PRI material is composed of two-dimensional (2-D) RH unit cells, while the ZRI material is realized by arranging 2-D RH and LH unit cells in a checkerboard tessellation [10], or by using only LH unit cells operated at the infinite wavelength frequency to give the zero-phase shift characteristic [11]. Note in [12] the LH unit cell used to implement ZRI material is based on the 2-D CRLH transmission line [12].

In this paper, a planar nine-way metamaterial power-combined amplifier is presented based on the power-divider structure of [11]. Due to its uniform isolation characteristics of the metamaterial power-dividing/combining structure, the graceful degradation performance of this power-combined amplifier is shown to be independent of the amplifier failure sequence.

In the following, Sec. II describes the design of a planar nine-way metamaterial power-combined amplifier. In Sec. III, circuit implementation and measured results are presented. The power combining of nine 1-W amplifiers gives an output power of 7.64 W with combining efficiency of 85% and power added efficiency (PAE) of 40% at 1.008 GHz [13]. The voltage-dividing/combining phenomenon is further experimentally verified through the field measurement at the node of each unit cell. Moreover, the graceful degradation performance of this nine-way power-combined amplifier is demonstrated via power and field measurements. Finally, Sec. IV gives the conclusion.

II. DESIGN

Fig. 1(a) shows the schematic of a planar nine-way metamaterial power-combined amplifier. The divider and combiner structures are composed of RH unit cells for PRI material and LH unit cells for ZRI material. The structures of RH and LH unit cells are shown in Fig. 1(b). The semi-circular interface between PRI and ZRI materials is approximated in a staircase manner. Each of the power divider and combiner includes 9 × 7 cells. Ports 1 and 2 located at the central RH unit cells of two PRI materials are the input and output ports, respectively. The remaining ports which are not indexed are open circuits. Nine amplifiers are located at the 8th column with their input and output ports connected to the LH unit cells at the 7th column and the 9th column, respectively.

A. Divider and Combiner

A nine-way power divider/combiner is designed on a 1.575-mm-thick RT/Duroid 5880 substrate with $\varepsilon_r = 2.2$ and $\tan\delta = 0.0009$. The operating frequency is 1 GHz. The

[1] This work was supported in part by the NSC under Grants 100-2221-E-002-225-MY3 and 101-2221-E-002-128-MY2.

Corresponding author:d95942009@ntu.edu.tw
DOI:10.6159/IJSE.2014.(4-1).79

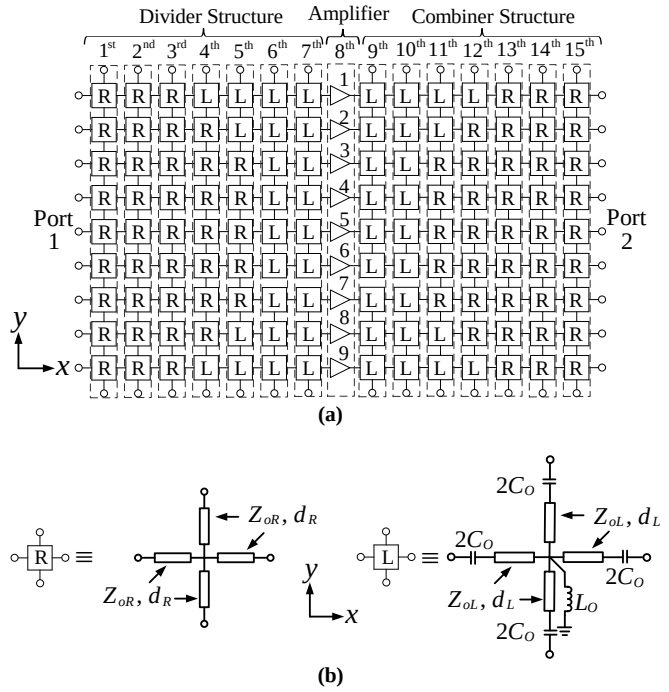

Fig. 1 (a) Schematic of a planar nine-way power-combined amplifier with (b) R and L representing RH and LH unit cells.

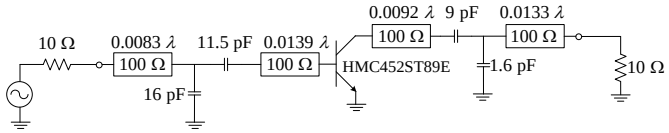

Fig. 2 Circuit schematic of an 1-W amplifier.

size of RH and LH unit cells is given by 10 mm × 10 mm, and the characteristic impedance $Z_{oR} = Z_{oL} = 100\ \Omega$. The length $2d_L$ of LH unit cell is 8 mm by considering the size of 0402 surface-mounted capacitor. By considering the parasitic effects of surface mounted device (SMD), MuRata 0603 36-nH SMD inductors and 0402 5.6-pF SMD capacitors are then used to realize LH unit cells with zero-phase shift characteristics.

B. Amplifier

The amplifiers used to develop this nine-way power-combined amplifier are Hittite HMC452ST89E GaAs InGaP HBT 1-W amplifiers. Fig. 2 shows the circuit schematic of an 1-W amplifier. The termination impedances are 10 Ω, which are obtained by calculating the input impedances of the LH unit cells at the 7th and 9th columns for the divider and combiner structures given in Fig. 1(a). The *S*-parameters, which are given for 1-W output power of this HBT amplifier, are then used to design the input and output conjugate matching circuits as shown in Fig. 2.

III. EXPERIMENTAL RESULTS

In this section, a planar nine-way metamaterial power-combined amplifier is presented and experimentally verified.

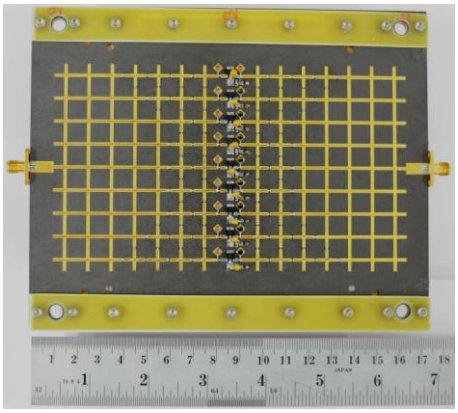

Fig. 3 Photograph of a planar nine-way metamaterial power-combined amplifier circuit.

The circuit is shown in Fig. 3. MuRata 0603 36-nH SMD inductors and 0402 5.6-pF SMD capacitors are used in the realization of LH unit cell. The shunt inductor of LH unit cell is placed upright in a hole drilled through the substrate. The amplifiers are Hittite HMC452ST89E 1-W power amplifiers.

A. Power Measurement

Fig. 4(a) shows the measured results of output power, power gain, and PAE of the nine-way power-combined amplifier at 1.008 GHz. The output power of 38.83 dBm at 1-dB gain compression point is obtained as the input power is 26.83 dBm, and the corresponding DC bias voltage and current are 5 V and 3.586 A to give a PAE about 40%. The power combining efficiency is 85%.

Three sequences of failed amplifiers are used to demonstrate the graceful degradation characteristic of this power-combined amplifier, as shown in Fig. 4(b). The failed amplifiers in each sequence are emulated by turning off the biases of corresponding operating amplifiers. The numbering and position of nine amplifiers can be observed from Fig. 1(a) and Fig. 3. In the first and second sequences, one, two, three, four, and five amplifiers are tuned off successively in an ordered manner and they are represented by (9, 5, 1, 3, 7) and (5, 4, 6, 3, 7), respectively. In the third sequence, two and four amplifiers are turned off successively and are represented by (1, 9, 2, 8). The ideal degradation characteristic of an *N*-way power-combined amplifier with *N* amplifiers being reasonably matched and having adequate isolation is given by [14]

$$\frac{P_{out}}{P_{out,max}} = (1 - \frac{m}{N})^2 \quad (1)$$

where P_{out} is the output power as *m* amplifiers fail and $P_{out,max}$ is the maximum output power as there is no amplifier failure. As shown in Fig. 4(b), compared to ideal results of (1), an additional power drop in each sequence is observed and shown increasingly as the number of failed amplifiers increases. It results from source and load mismatches of the remaining operating amplifiers. Note, the amplifiers are matched only as nine identical excitations are

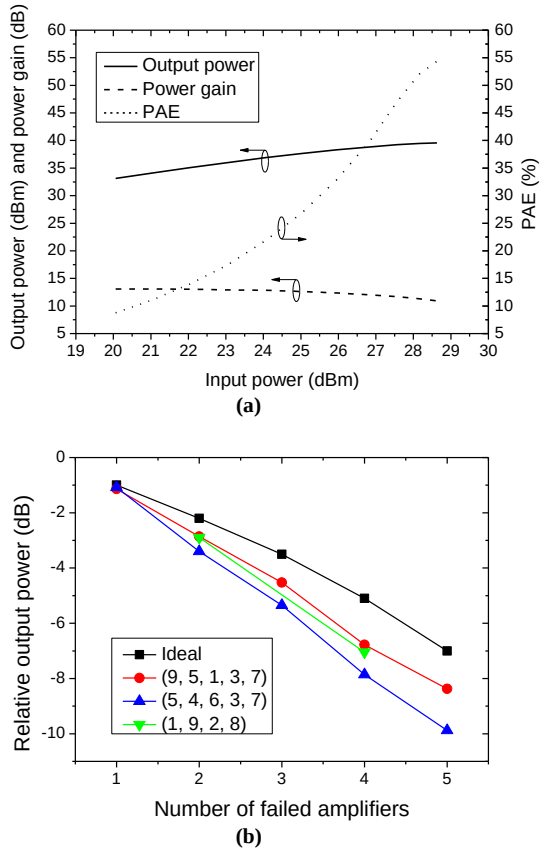

Fig. 4 Measured results of (a) the output power, power gain, and PAE and (b) the output power degradation at 1.008 GHz.

at the input ports of combiner for the termination impedances of 10 Ω. It is then different from that of using radial [3], [4] power dividers and combiners, which have isolation resistors to retain matched inputs and outputs for the remaining operating amplifiers.

In addition, as shown in Fig. 4(b), due to port-independent isolation characteristics for both power divider and combiner, similar graceful degradation characteristics for these three sequences of failed amplifiers are observed. A slightly better performance for the first and third sequences than that of the second sequence may be due to non-uniformity of nine amplifiers. Note, the results given in Fig. 4(b) are different from those observed in [3], which is dependent on the specific sequence of failed amplifiers due to port-dependent isolation characteristics of radial power-dividing/combining structures.

B. Field Measurement

To further demonstrate its dividing/combining and graceful degradation phenomena of this power-combined amplifier, measured spatial voltage distributions near the central node of each RH and LH unit cells over the structure are presented. Fig. 5 shows the field measurement arrangement to acquire the voltage distribution at each cell. The circuit is supported by four stainless steel rods on an optical table with a height about 15 cm. An Agilent N5230A

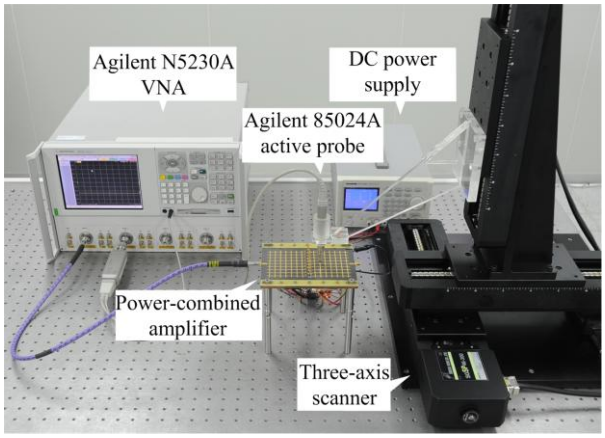

Fig. 5 Photograph of the field measurement arrangement.

vector network analyzer (VNA) is used in two-port measurement mode. Its port 1 is connected to the port 1 of the power-combined amplifier, and the VNA port 2 is connected to an Agilent 85024A active probe. The probe scans on the surface near the central node of each unit cell through a Sigma-Koki SGSP 46-300 three-axis scanner. A personal computer controls the VNA and the scanner through GPIB and RS-232 interfaces.

Fig. 6 shows the active probe measured results of S_{21} from VNA at 1.008 GHz. Note, results on the left side of the 1st column and the right side of the 14th column show the effects near the SMA connectors at input and output ports, respectively. The excitation source at the 5th row and the 1st column gives $|S_{21}| = -1.1$ dB, and $|S_{21}|$ values along the 5th row for the 7th, 8th, and 14th columns are -6 dB, 0 dB, and 7.1 dB, respectively. Note, results of the 7th column and the 8th column show the voltage distribution near the power divider output ports and the combiner input ports respectively, and the amplification of voltage magnitude is shown from the 7th column to the 8th column. It demonstrates not only the similar voltage dividing and combining characteristics, but also the voltage-dividing/combining phenomenon within the power divider and combiner. Moreover, as shown in Fig. 6(b), a cylindrical wavefront is formed in PRI material then is converted to a planar wavefront in ZRI material.

Furthermore, the active probe measured results of $|S_{21}|$ in accordance with Fig. 4(b) for the third sequence as an example are presented in Fig. 7. It is useful not only for the verification of graceful degradation characteristic but also for the circuit diagnosis. As shown in Fig. 7, from column 8 to column 14, the $|S_{21}|$ distribution is shown to decrease gradually with the number of failed amplifiers, and the degradation characteristics of $|S_{21}|$ at the output port are similar to the results given in Fig. 4(b). By observing the 8th column, $|S_{21}|$ at those rows with operating amplifiers is shown obviously higher than that of those rows with failed amplifiers to indicate not only a proper isolation among the nine amplifiers but also the usefulness for identifying the

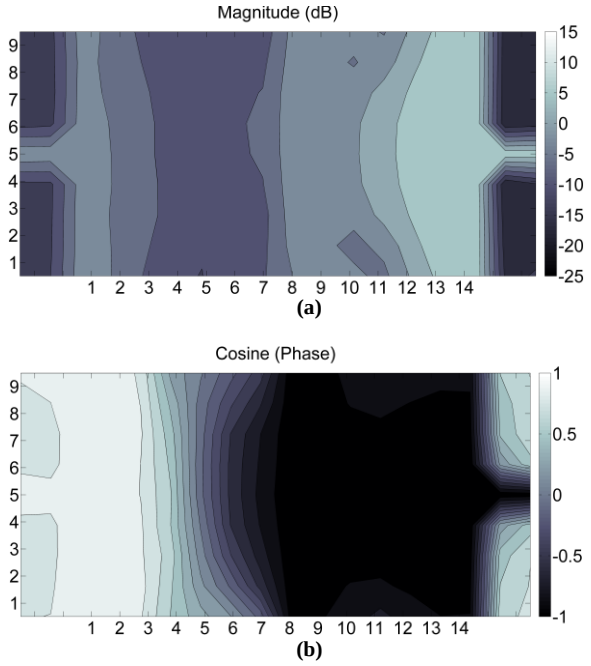

Fig. 6 Active probe measured results of S_{21} with (a) magnitude in dB with respect to the input port and (b) cosine(phase).

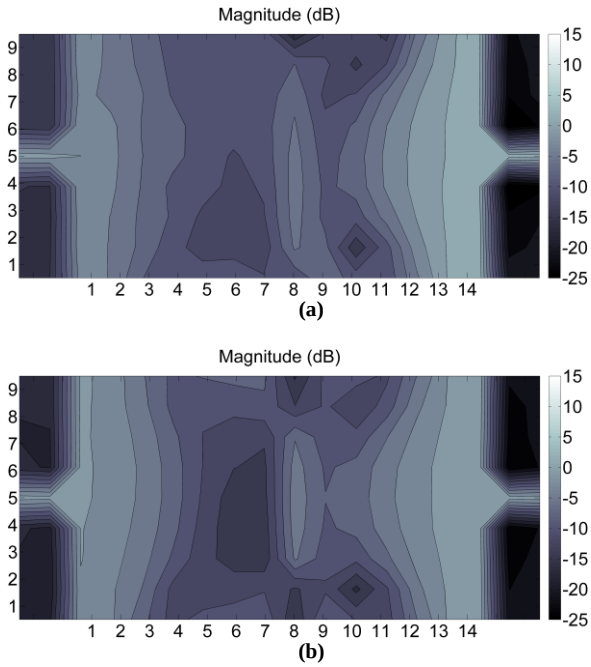

Fig. 7 Active probe measured results of $|S_{21}|$ with respect to the input port for the third sequence (1, 9, 2, 8) with (a) two and (b) four failed amplifiers.

failed amplifiers distribution in practical circuit diagnosis. Moreover, the reflection due to mismatched amplifiers can be clearly observed from the non-uniform $|S_{21}|$ distribution in ZRI material. Note, as the positions of failed amplifiers in the power-combined amplifier are arranged in a symmetric manner, the $|S_{21}|$ distribution within power-combined amplifier structure is shown to have a line of symmetry along the 5th row, as shown in Fig. 7.

IV. Conclusion

This paper presents the measurements of a planar nine-way power-combined amplifier based on the metamaterial power-dividing/combining structure composed of PRI and ZRI materials. The power combining of nine 1-W amplifiers attains an output power of 7.64 W with a combining efficiency of 85% and a PAE of 40% at 1.008 GHz. The graceful degradation characteristic of this nine-way power-combined amplifier is experimentally demonstrated via power and field measurements and shown differently as that of using radial power dividers and combiners.

References

[1] K. J. Russell, "Microwave power combining techniques," *IEEE Trans. Microw. Theory Tech*., vol. MTT-27, no. 5, pp. 472–478, May 1979.

[2] E. Wilkinson, "An N-way hybrid power divider," *IRE Trans.Microw. Theory Tech*., vol. MTT-8, no. 1, pp. 116–118, Jan. 1960.

[3] J. M. Schellenberg and M. Cohn, "A wideband radial power combiner for FET amplifiers," in *IEEE Int. Solid-State Circuits Conf*., Feb. 1978, pp. 164–166.

[4] A. E. Fathy, S. W. Lee, and D. Kalokitis, "A simplified design approach for radial power combiner," *IEEE Trans. Microw. Theory Tech*., vol. 54, no. 1, pp. 247–255, Jan. 2006.

[5] R. J. Mohr, "A microwave power divider," *IRE Trans. Microw. Theory Tech*., vol. MTT-9, no. 6, p. 573, Nov. 1961.

[6] S. Mizushina, "2^n oscillators combined with 3-dB directional couplers for output power summing," *Proc. IEEE*, vol. 55, no. 12, pp. 2166–2167, Dec. 1967.

[7] C. Caloz and T. Itoh, *Electromagnetic Metamaterials: Transmission Line Theory and Microwave Applications*, New York: Wiley, 2005.

[8] A. Lai, T. Itoh, and C. Caloz, "Composite right/left-handed transmission line metamaterials," *IEEE Microw. Mag*., vol. 5, no. 3, pp. 34–50, Sep. 2004.

[9] A. Lai, K. M. K. H. Leong, and T. Itoh, "A novel *N*-port series divider using infinite wavelength phenomena," in *IEEE MTT-S Int. Microw. Symp. Dig*., June 2005, pp. 1001–1004.

[10] K. W. Eccleston, "Planar *N*-way metamaterial power divider," in *Proc. Asia-Pacific Microw. Conf. Dig*., Dec. 2009, pp.1024–1027.

[11] W. C. Lee and T. H. Chu, "Design and measurement of a planar 9-way metamaterial power divider," in *IEEE MTT-S Int. Microw. Symp. Dig*., June 2012, pp. 1–3.

[12] G. V. Eleftheriades, A. K. Iyer, and P. C. Kremer, "Planar negative refractive index media using periodically *L-C* loaded transmission lines," *IEEE Trans. Microw. Theory Tech*., vol. 50, no. 12, pp. 2702–2712, Dec. 2002.

[13] W. C. Lee and T. H. Chu, "Design and power performance measurement of a planar metamaterial power-combined amplifier," *IEEE Trans. Microw. Theory Tech*., vol. 61, no. 6, pp. 2414–2424, June 2013.

[14] R. L. Ernst, R. L. Camisa, and A. Presser, "Graceful degradation properties of matched *N*-port power amplifier combiners," *in IEEE MTT-S Int. Microw. Symp. Dig*., June 1977, pp. 174–177.